

to the four measured curves for HMS and HTS fibres, where the assigned property values of Table I normalized to measured control values are shown by the X's in Figs. 1 and 2. It is interesting to note that with higher levels of radiation exposure in air than have been obtained at present, the sheaths of HMS fibres should eventually be so weakened by oxidation that the fibres would begin to undergo sheath-initiated failure, and according to the assigned values of Table I this failure regime was almost reached. When this occurs, the HMS strength of Fig. 1 should then begin to decrease rapidly with additional radiation exposure, and the strain curve of Fig. 3 after reaching a maximum should then begin to fall off once again.

Based on what has been said to this point, one should expect the strength of HMS fibres irradiated in LN_2 to remain fairly constant and the modulus to continue increasing beyond the maximum value for an air irradiation, but instead they decrease. The lower-than-expected values here are also thought to be caused by the sheath and core structure of the HMS fibre, however, but this is thought to be the result of a radiation-enhanced temperature effect rather than a radiation effect alone. Radiation energy is stored in graphite crystallites of fibres as a result of displaced lattice atoms [13], and this "Wigner energy" [14] begins to be released in the form of heat when the temperature is raised to the point where displaced carbon atoms become mobile and re-enter vacant lattice sites. When carbon fibres irradiated to a fast-neutron fluence of 3×10^{18} n/cm² were lifted out of LN_2 into the dense nitrogen vapour ($\sim -140^\circ\text{C}$) immediately above the liquid level, this release of stored energy was sufficient to very rapidly raise the temperature of the fibres to more than 175°C . The fibres, which before warming had been stiffened by radiation exposure in LN_2 , it is supposed, then cooled off very rapidly in the gaseous nitrogen; it is felt that the resulting

thermal shock on the HMS fibre, with its widely different coefficients of thermal expansion for the sheath and core of the fibre, caused additional damage to the already-flawed fibre which resulted in reduced strength and modulus. The more uniform HTS fibre was evidently able to withstand this thermal shock without being damaged. All reported radiation-effects data, then, seem to be explainable by displacement-oxidation competition in conjunction with a flawed-core model for HMS fibres.

References

1. B. F. JONES, 10th Biennial Conf. on Carbon (June 1971). Summary of Papers p. 190.
2. B. F. JONES and R. G. DUNCAN, *J. Mater. Sci.* **6** (1971) 289.
3. B. F. JONES, *ibid.* **6** (1971) 1225.
4. B. L. BUTLER and R. J. DIEFENDORF, 9th Biennial Conf. on Carbon (June 1969). Summary of Papers p. 161.
5. R. E. BULLOCK, *Rad. Effects* **11** (1971) 107.
6. *Idem, ibid*, in press.
7. S. ALLEN, G. A. COOPER, and R. M. MAYER, *Nature* **224** (1969) 684.
8. G. A. COOPER and R. M. MAYER, *J. Mater. Sci.* **6** (1971) 60.
9. B. F. JONES and I. D. PEGGS, *J. Nucl. Mater.* **40** (1971) 141.
10. J. W. JOHNSON, Applied Polymer Symposia No. 9 (1969) 229.
11. C. W. LEMAISTRE and R. J. DIEFENDORF, 10th Biennial Conf. on Carbon (June 1971). Summary of Papers p. 163.
12. L. E. MURR and O. T. INAL, *J. Appl. Phys.* **42** (1971) 3487.
13. R. W. CAHN and B. HARRIS, *Nature* **221** (1969) 132.
14. M. BURTON and T. J. NEUBERT, *J. Appl. Phys.* **27** (1956) 557.

Received 24 January and
accepted 21 April 1972

R. E. BULLOCK
General Dynamics, Convair Aerospace Division
Fort Worth, Texas 76101, USA

A new contribution to the equilibrium diagram of the Cu-Se system

The latest systematic examination of the copper-selenium equilibrium diagram has been reported by Heyding [1]. In the range where non-stoichiometric cuprous selenide Cu_{2-x}Se is stable, measurements have been carried out above 80°C only and so the phase relations at lower

temperatures are as yet unknown. In this work we used some of the results which we obtained in our general investigations of the semi-conducting properties of non-stoichiometric cuprous selenide, i.e. those which are suitable for construction of the unknown part of the equilibrium diagram. In fact, this work is a logical extension of our recent paper about the relation between the electrical conductivity and

phase-transformations of non-stoichiometric Cu_{2-x}Se [2]. In the latter work we showed that Cu_{2-x}Se may be considered as a solid solution of Se in stoichiometric Cu_2Se , which means that the equilibrium diagram is divided by two lines into three regions: a region where only the high-temperature, cubic, β -phase is present; a region where the β -phase and the α -phase exist simultaneously; and a region where only the low-temperature, non-cubic, α -phase is present. This equilibrium diagram was later confirmed by microhardness measurements [3]. Further, the phase-transition may be considered as being always in equilibrium, even at fairly fast heating or cooling rates, because the diffusion of copper ions in cuprous selenide is unusually fast.

These two considerations made it possible to work out a simple physical model which, for the temperature-dependence of conductivity in the two-phase region, gives a characteristically unsymmetrical, "pocket-like" curve. Our present work uses the same physical model. However, for measurements of electrical conductivity we used samples with a considerably greater content of Se, treated at much lower temperatures.

The samples of non-stoichiometric cuprous selenide were prepared by means of direct synthesis from pure and precisely weighed components in an evacuated and sealed quartz tube. The initial composition $(2-x)$ was determined from the masses of the components used in the synthesis. Since the composition of

each sample was varied by selective evaporation of Se [4], electrical conductivity was measured throughout on one and the same sample, though each time with a different value of $(2-x)$. The composition was varied from 36.77 at. % Se ($\text{Cu}_{1.720}\text{Se}$) to 35.41 at. % Se ($\text{Cu}_{1.824}\text{Se}$), and electrical conductivity was measured at temperatures ranging from -212 to $+80^\circ\text{C}$. The heating or cooling rate was 2 deg/min, which is sufficiently slow to assure an equilibrium condition [2].

The dependence of electrical conductivity on temperature for the sample with 36.36 at. % Se ($\text{Cu}_{1.750}\text{Se}$) is shown in Fig. 1. The measurements gave a curve of the same shape for every sample, regardless of its composition within the mentioned range. Of course, the absolute value of conductivity and the positions of the characteristic temperature arrests of curves change from sample to sample. As in the earlier work [2], the characteristic "pocket"-like curve between T_α and T_β , denoting the beginning and the end of the two-phase region of non-stoichiometric Cu_{2-x}Se , was observed in the present work as well.

A comparison of the curves for samples with a different composition will show that the difference $(T_\beta - T_\alpha)$ decreases as the fraction of Se changes from 35.41 at. % Se to higher values. Since T_α remains constant (-103°C), we conclude that eutectic transformation is taking place. As can be seen in Fig. 2, our experimental points between 35.41 at. % Se ($\text{Cu}_{1.824}\text{Se}$) and 36.20 at. % Se ($\text{Cu}_{1.763}\text{Se}$) tie up perfectly with the diagram published earlier [2]. The rapid decrease of conductivity below temperature T_α may be attributed to the eutectic elimination of some other phase which is richer in Se. For samples with a composition near 36.30 at. % Se ($\text{Cu}_{1.755}\text{Se}$) the temperature T_β is very close to temperature T_α . At the same time the conductivity minimum between T_α and T_β is hardly perceptible. In the case of an ideal eutectic composition, T_α would be equal to T_β and the conductivity minimum between these two temperatures would disappear. Thus, the value of T_β could not be accurately established in this region. The difference between T_β and T_α increases again above 36.30 at. % Se. The temperature T_α still remains constant. Of course, in this part of the equilibrium diagram we had to take into account the presence of an increasing amount of some other phase, different from Cu_{2-x}Se . For this reason the diffusion processes

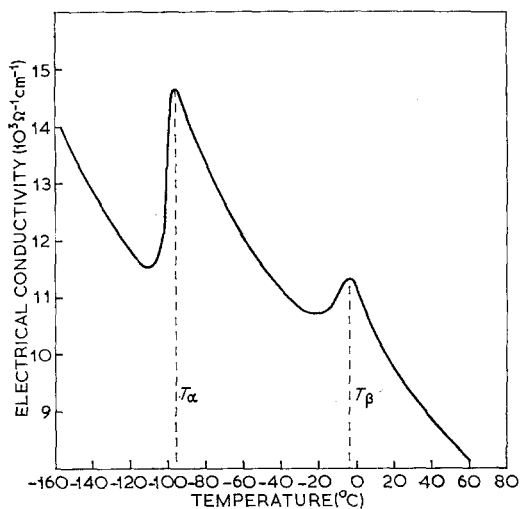


Figure 1 Electrical conductivity of $\text{Cu}_{1.750}\text{Se}$ sample.

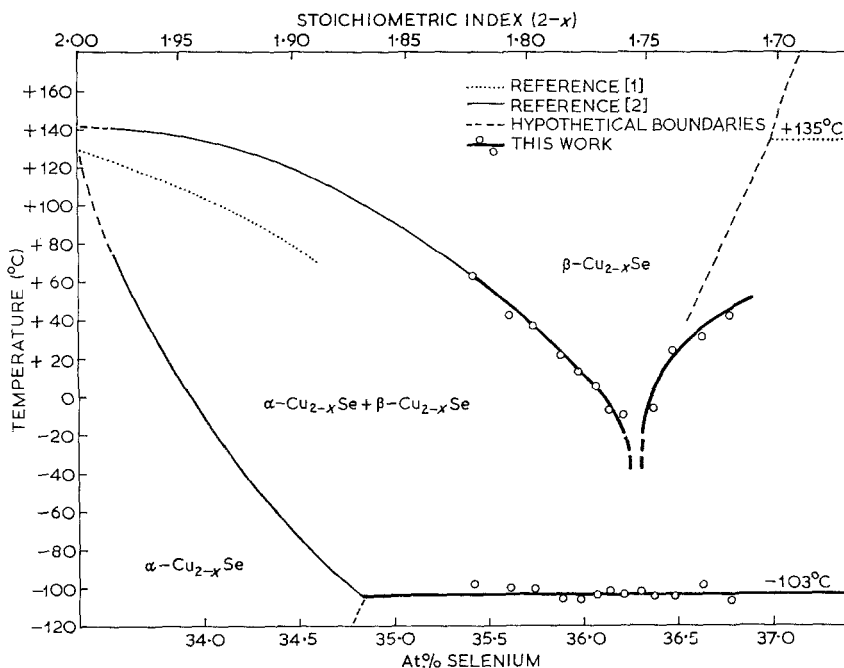


Figure 2 Equilibrium diagram of the Cu-Se system.

are not so rapid that the heating and cooling of samples during measurements could be considered as maintaining complete equilibrium. Therefore this part of the equilibrium diagram is established with less precision. In any case this other phase is not Cu_3Se_2 but, more likely, CuSe . This is in agreement with Heyding's observation [1] that in samples which have once been heated above 135°C , Cu_3Se_2 no longer appears.

The homogeneity range of the cubic or high-temperature phase of Cu_{2-x}Se at room-temperature (26°C) determined by means of measurements of electrical conductivity ($\text{Cu}_{1.79}\text{Se}$ – $\text{Cu}_{1.73}\text{Se}$) is not in agreement with the range determined from X-ray measurements ($\text{Cu}_{1.82}\text{Se}$ – $\text{Cu}_{1.75}\text{Se}$) [1]. In view of the drastic and easily measurable changes in conductivity at temperature T_x we must conclude that electric conductivity supplies more reliable information.

References

1. R. D. HEYDING, *Canad. J. Chem.* **44** (1966) 1233.
2. Z. OGORELEC and B. ČELUSTKA, *J. Phys. Chem. Solids* **30** (1969) 149.
3. Z. OGORELEC, R. ROČAK, and J. IVIĆ, *Phys. Stat. Sol. (a)* **6** (1971) K29.
4. B. ČELUSTKA and Z. OGORELEC, *Croat. Chem. Acta* **41** (1969) 73.

Received 7 February and
accepted 21 March 1972

Z. OGORELEC
B. MESTNIK
D. DEVČIĆ
*Institute of Physics
University of Zagreb
Yugoslavia*

On the amplitude-independent internal friction in crystalline solids

Recent work on the background internal friction in alkali halides [1], high-purity copper [2] and alpha-brasses [3], has established the inapplicability of the Granato-Lücke model to the results,

over a wide frequency spectrum. To explain the observed features, the depth and coherency of the internal microstress-fields have to be taken into account [4]. In this note we present new measurements of the background internal friction in high-purity brass polycrystals containing from 0.1 to 5 at% of zinc. These results